Angle-resolved photoemission study of thin molecular-beam-epitaxy-grown α-Sn$_{1-x}$Ge$_x$ films with $x \sim 0.5$

Hartmut Höchst, Michael A. Engelhardt, and Isaac Hernández-Calderón[*]

Synchrotron Radiation Center, University of Wisconsin–Madison, Stoughton, Wisconsin 53589-3097

(Received 28 February 1989; revised manuscript received 3 August 1989)

Angle-resolved synchrotron-radiation photoemission spectroscopy is used to study the electronic structure of metastable epitaxial films of α-Sn$_{1-x}$Ge$_x$ alloys. Homogeneous crystalline alloy films were grown by molecular-beam epitaxy on Ge(100) substrates at $\sim 400\,°C$ up to a thickness of ~ 300 Å. Photoemission core-level analysis indicates a strong tendency to form a compound with a composition close to $x \sim 0.5$. Angle-resolved spectra show a shift of the Γ_8 valence band from ~ 0.6 eV in Ge(100) to ~ 0.16 eV below E_F in the α-Sn$_{0.48}$Ge$_{0.52}$ alloy. The experimental information of a constant alloy Fermi level locates the top of the Γ_8 valence band ~ 0.16 eV below E_F. Assuming a linear band model, the direct band gap of $E_g \sim 0.2$ eV for $x \sim 0.5$ will then locate the bottom of the Γ_7 conduction band ~ 0.04 eV above E_F.

I. INTRODUCTION

Alloying the semimetal α-Sn with Ge is expected to open the symmetry-induced zero band gap of α-Sn.[1] Assuming a linear relationship between the band structure of both components, the direct band gap $E_g(\Gamma_7 - \Gamma_8) = -0.413$ eV would be zero and reverse the order of these bands at a Ge concentration of $x \sim 0.35$. Further increase of Ge would open a direct gap with a maximum value of $E_g \sim 0.55$ eV at room temperature for $x \sim 0.78$. For Ge concentrations larger than 0.78 the gap should then be indirect from Γ_8 to L_6, with E_g ranging from 0.55 to 0.66 eV for pure Ge.

Alloys in the compositional range of $x \sim 0.35 - 0.78$ would allow the band-gap properties to be tailored over a range of great technological interest. Due to the lack of polar scattering in α-Sn$_{1-x}$Ge$_x$ alloys, the mobilities may be considerably higher than those of the isoelectronic Hg$_{1-x}$Cd$_x$Te system. If it is feasible to prepare an ordered α-Sn$_{0.5}$Ge$_{0.5}$ compound, the carrier mobilities may improve even further by quenching alloy scattering.

Unfortunately the α phase of bulk Sn is only stable below 13.2 C.[2] Thin films of α-Sn grown heteroepitaxially on CdTe and InSb, however, are substrate stabilized with α-β transition temperatures well above 100 °C.[3-7] One may speculate that the addition of Ge may help to raise the phase-transition temperature even further.[3,8] Assuming a simple linear relationship between the α-β transition temperatures for $T_{Sn} = 13.2\,°C$ and $T_{Ge} = 932.5\,°C$ the alloy transition temperature would increase by $\sim 9\,°C/at.\%$ Ge.

Recent low-temperature transport measurements indicated good electronic quality of molecular-beam-epitaxy (MBE) grown α-Sn and α-Sn$_{1-x}$Ge$_x$ alloys.[9,10] Films of α-Sn up to 5000 Å thick showed n-type behavior with $n_d \sim 3 \times 10^{17}$ cm^{-3} and mobilities of several times 10^4 cm^2/V sec.[10] These studies also indicated a small strain-induced shift of the L_6 conduction band which was opposite to the direction to be expected from a linear alloy band-structure model.

The existence of larger lattice mismatch will be an additional disadvantage and may contribute to the instability of the metastable α phase of Sn$_{1-x}$Ge$_x$ alloys. Conventional growth techniques working under thermodynamic equilibrium are thus not suitable for the fabrication of the metastable α-Sn$_{1-x}$Ge$_x$ alloys. Using an Ar-ion-assisted dc-diode sputter technique Shah et al.[11] prepared alloy films containing up to 15 at. % Sn. Films with 8 at. % Sn grown on Ge(100) and GaAs(100) were single crystalline, while those grown on amorphous glass substrates were polycrystalline but still single phased for Sn concentrations as high as 15%. Other sputter deposition experiments[12-14] produced amorphous alloys up to $x \sim 0.5$ with tetrahedrally coordinated Sn and β-Sn clusters. Depending on the growth conditions, Sn atoms were either randomly bonded or solely bonded to nearest-neighbor Ge atoms. Small-angle x-ray scattering showed very good mixing on an atomic scale for amorphous SnGe compound films.[12] With appropriate substrates and optimized growth conditions it appears to be possible to prepare epitaxial, tetrahedrally bonded, thin alloy films and to minimize or prevent the formation of metallic β-Sn precipitates over a wide compositional range.

We report first results of a photoemission study to grow α-Sn$_{1-x}$Ge$_x$ films with MBE on Ge(100). Reflection high-energy electron diffraction (RHEED) and *in situ* angle-resolved synchrotron-radiation photoemission spectroscopy (ARPES) was used to investigate the growth and electronic valence-band structure of single phase alloy films grown at $\sim 400\,°C$ on Ge(100). Core-level intensity measurements indicate a strong tendency for the growth of alloys with $x \sim 0.5$.

II. EXPERIMENTAL

Polished Ge(100) plates, 10×10 mm^2 and ~ 1 mm thick, were used as substrate material for the MBE growth of the α-Sn$_{1-x}$Ge$_x$ alloys. The substrates were cleaned with organic solvents and rinsed with deionized

water before they were inserted into the MBE system. Prior to the growth, the Ge surface was further cleaned by sputtering with Ar ions of 500 eV energy. Annealing for 10 min at $\sim 600\,°C$ removed crystal damage which was caused by the sputtering process or by the cutting and polishing procedure. The surface structure was monitored by RHEED with an electron energy of $E_0 \sim 25$ keV. The sample could be rotated by $\sim 220°$ around the surface normal, which allowed us to take RHEED pattern along several high-symmetry azimuths.

The sputter annealing process produced clean and ordered surfaces which gave a well-resolved RHEED pattern typical for a 2×1 reconstructed Ge(100) surface.[15,16] It should be noted that the 2×1 structure, which is generally believed to be formed by dimers, is not the only possible reconstruction for Ge(100) surfaces. Higher-order reconstructions such as $c(2 \times 4)$ and $p(2 \times 2)$ can also be obtained through an order-disorder phase transition at lower temperatures.[17,18]

We tried to further improve the surface quality by growing Ge buffer layers on the sputter annealed Ge(100) substrates. Based on the RHEED pattern and on valence-band stuctures in the ARPES, Ge buffer layers grown at 400–470 °C up to 100 nm thick do not seem to significantly increase the surface quality of sputter annealed Ge(100) surfaces.

Tin and germanium were evaporated out of boron nitride crucibles from liquid-nitrogen-shrouded effusion cells. Deposition rates were measured with a calibrated and temperature-stabilized quartz crystal thickness monitor. At cell temperatures of $\sim 1200\,°C$ typical growth rates were ~ 2–5 Å/s. Both source materials had a purity of 99.9999%.

Photoemission experiments were performed in situ utilizing synchrotron radiation generated by the University of Wisconsin's electron storage ring ALADDIN. The synchrotron radiation was monochromatized with a Seya-Namioka-type monochromator which delivered photons in the range $h\nu = 10$–38 eV, and in a separate set of experiments with a 6-m torroidal grating monochromator (TGM) which produced photons up to $h\nu = 200$ eV. The synchrotron radiation was p polarized along the [110] direction with an angle of incidence of 60° with respect to the surface normal. Photoelectrons were collected at normal emission. The total experimental energy resolution of the photoemission-spectrometer–optical-monochromator system as determined from the width of the Fermi level emission of a metallic substrate was ~ 0.18 eV in the lower photon energy range and increased to ~ 0.35 eV for $h\nu \sim 100$ eV.

III. RESULTS AND DISCUSSION

Figure 1 shows a set of valence-band photoemission spectra which we obtained exposing a Ge(100) substrate at different temperatures to a mixed molecular beam originating from individual Sn and Ge molecular-beam sources. The data shown in Fig. 1 result from a flux ratio of $n_{Sn}/n_{Ge} = 3$. Assuming a unit sticking coefficient for both source materials, the offered flux ratio should deposit a film containing 25 at. % Ge. Based on Sn $4d$ and Ge
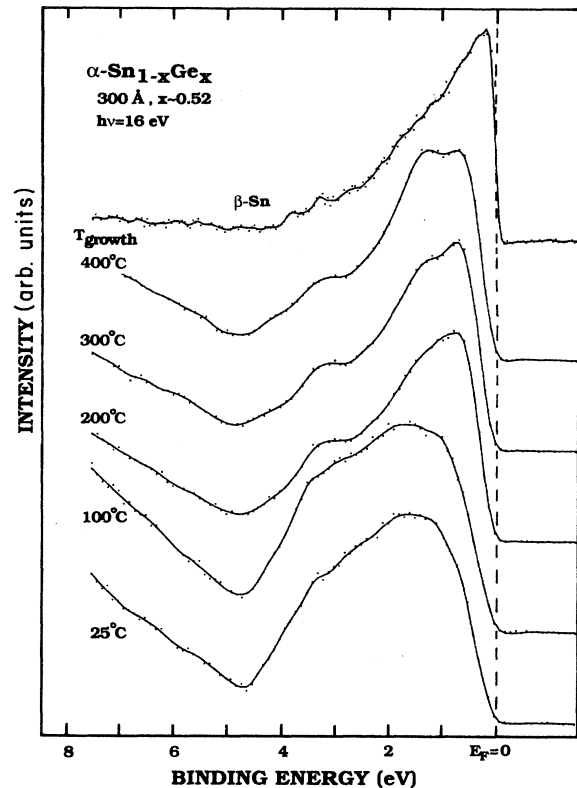

FIG. 1. Normal-emission valence-band spectra of α-$Sn_{0.48}Ge_{0.52}$ grown on Ge(100) as a function of growth temperature. The top spectrum corresponds to a film of β-Sn showing a Fermi edge emission which is characteristic for a metal.

$3d$ photoemission intensities of the deposited alloys [which were normalized to those of pure α-Sn and Ge(100) surfaces] we determined the composition of the deposited material with an estimated accuracy of $\pm 5\%$. Our core-level analysis indicates a significant compositional deviation in the deposited films compared to that of the molecular beams. The aspect of different MBE incorporation efficiencies of not of importance at this point but will be discussed later in the paper.

With increasing deposition temperature the valence-band spectrum changes from a broad unstructured feature into a three-peak spectrum. Growth at 200 °C clearly shows the onset of sharper structures which develop further at higher growth temperatures. However, it is interesting to note that, contrary to the alloy growth on CdTe substrates,[19] even at low growth temperatures there is no indication for a precipitation of the metallic β-Sn phase. The alloy valence-band spectra do not show the typical Fermi-level emission of a β-Sn film which is also shown in Fig. 1.

Higher substrate temperatures increase the surface mobility and allow a much smoother film growth. For growth temperatures above 200 °C the spotty RHEED pattern is basically free of structures typical for polycrystalline overlayer. With higher substrate temperatures we also observe sharper direct transition structures increas-

ing in the angle-resolved photoemission spectra. Since direct (k conserving) transitions strongly depend on the absence of surface scattering their relative intensity increase can also be used as indirect evidence of the improved crystalline order.[20,21]

Since films with a thickness of up to 300 Å show still a large degree of order and relatively sharp transitions, they were used to determine the bulk electronic structure by ARPES. The presence of compressive overlayer strain caused by ~6.5% lattice mismatch for an alloy with $x \sim 0.5$ is most likely the main reason for the observed surface roughening after the deposition of the first few monolayers. With our present data it is not possible to correctly determine a critical film thickness. RHEED patterns as well as ARPES spectra support the existence of ordered alloy films up to ~300 Å. These thicknesses are at least an order of magnitude larger than what can be expected from a model based on the balance of strain and dislocation nucleation energy.[22] The α-$Sn_{1-x}Ge_x$ system may need a more refined theory including microscopic thermodynamic functions of the overlayer which is a complex calculation out of the scope of the present work.

Figure 2 shows a set of normal emission spectra measured at different photon energies. With increasing pho-
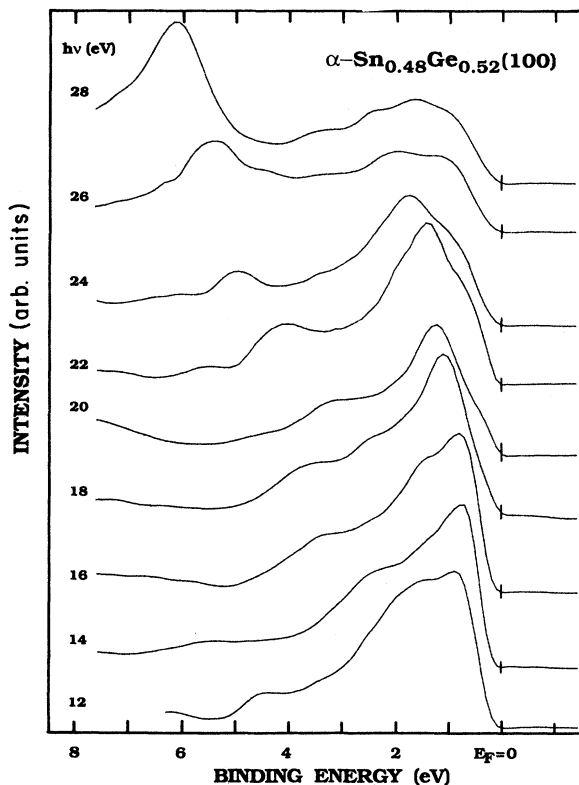

FIG. 2. Normal-emission valence-band spectra of a 200-Å-thick α-$Sn_{0.48}Ge_{0.52}$ film grown at 400 °C showing the dispersion of the initial states as a function of photon energy.

ton energies, emission features show considerable dispersion across the valence band. Comparing these spectra to those of clean Ge(100), it is easy to relate the strong peaks to direct transitions from the light-hole and split-off valence bands. Emission from the 2 valence band starts at ~1.5 eV for $h\nu = 16$ eV and disperses to ~6.2 eV for $h\nu = 28$ eV. We did not attempt to perform a detailed band mapping of these lower-lying valence bands but it should be noted that the alloy spectra follow closely the experimental[16] as well as the calculated[23] dispersion of the Ge valence bands along the ΓX direction.

This observation indicates that alloying Ge with Sn causes only minor changes of the deeper electronic valence-band structure. However, differences of the alloy electronic structure are present at the region close to the valence-band maximum. At $h\nu \sim 20$ eV the alloy spectrum shows a weaker emission feature slightly below the Fermi level which has no counterpart in the spectra of the clean Ge(100) surface. The shift in photon energy of the Γ_8 emission in Ge(100) from $h\nu \sim 14$ to 20 eV for the same transition in the Sn/Ge alloy, is too large to be solely accounted for by a change of the inner potential U_0 of the final-state bands.[24,25] It is known that the final-state dispersion deviates considerably from the free-electron parable at lower kinetic energies near the Brillouin zone inflection points. Final-state bands have been successfully fitted to experimental data of e.g., GaAs[26] with a reduced effective mass $m^* \sim 0.2$ m_e. A detailed band mapping analysis of the ARPES around the Γ_8 emission certainly requires the deviations from the free-electron behavior to be taken into account. For the purpose of the present paper however, we do not feel the need to address this issue further.

A closer look at the photoemission spectra around the region of the valence-band maximum is given in Fig. 3. The comparison with the valence spectra of clean Ge (dashed lines) clearly shows the additional alloy emission in the gap region. For $h\nu = 16$ eV, the top of the alloy valence-band spectrum shows a significant shift towards E_F which develops at $h\nu \sim 20$ eV to a pronounced shoulder centered ~0.16 eV below the Fermi level. For higher photon energies the valence-band peak disperses away from E_F.

The dispersion of lower-lying valence bands of the α-$Sn_{1-x}Ge_x$ alloy follows closely that of Ge for larger k values along ΓX. Closer to the top of the valence bands both materials show significant differences. Since the closest feature to the Fermi level is observed for the alloy at ~0.16 eV for $h\nu = 20$ eV and the Ge $3p$ core level did not show shifts related to band bending effects, we can assume that the emission ~0.16 eV below E_F is due to transitions from the top of the alloy valence band. The observed emission is thus an indication of the expected narrowing of the alloy band gap. Assuming a linear behavior between the Γ_8 valence band and the Γ_7 conduction band, the direct energy gap for an alloy with $x = 0.48$ would be ~0.2 eV. Using the additional experimental information of a constant Fermi level, we can then assign the position of the conduction-band minimum to be ~0.04 eV above E_F.
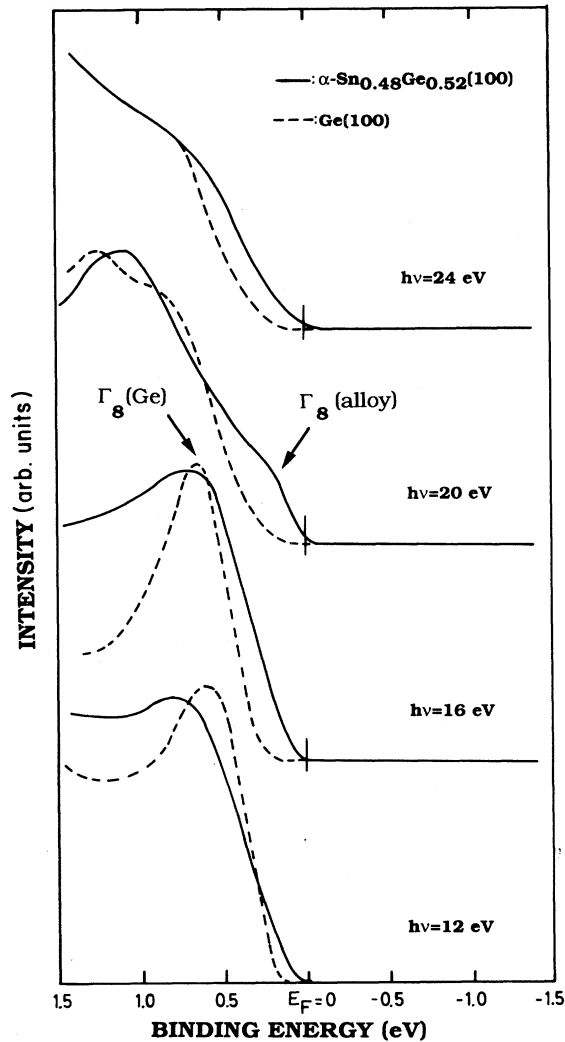
FIG. 3. Comparison between the normal-emission spectra of Ge(100) and α-Sn$_{0.48}$Ge$_{0.52}$ around the top of the valence band. The narrowing of the gap in the alloy film is evident from the emission originating from states of the Γ_8 valence band at $h\nu \sim 20$ eV.

FIG. 4. Work function measured from the photoemission cutoff spectrum of α-Sn, a 200-Å film of α-Sn$_{0.48}$Ge$_{0.52}$ and Ge(100). The presence of metallic Sn clusters or a phase separation of the alloy into α-Sn and Ge would appear as steps in the low-energy side of the spectrum.

Our experimental data shown in Fig. 3 indicate that it is possible to prepare thin ordered crystalline films of α-Sn$_{1-x}$Ge$_x$ alloys without detectable β-Sn precipitations by MBE on Ge(100) substrates. However, one may argue that the minor differences between the photoemission spectra of the alloy and those of Ge(100) are caused by the precipitation of Sn droplets floating on top of the Ge substrate. The possibility of that happening is certainly large, keeping in mind that the alloys is a thermodynamic unstable bulk system where both components are nearly insoluble in each other. Nevertheless, the absence of a Fermi-level emission and Sn $4d$ core-level spectra which showed a small energy shift compared to the metallic β-Sn phase led us to assume that Sn and Ge are homogeneously mixed in our thin alloy films. The only noticeable
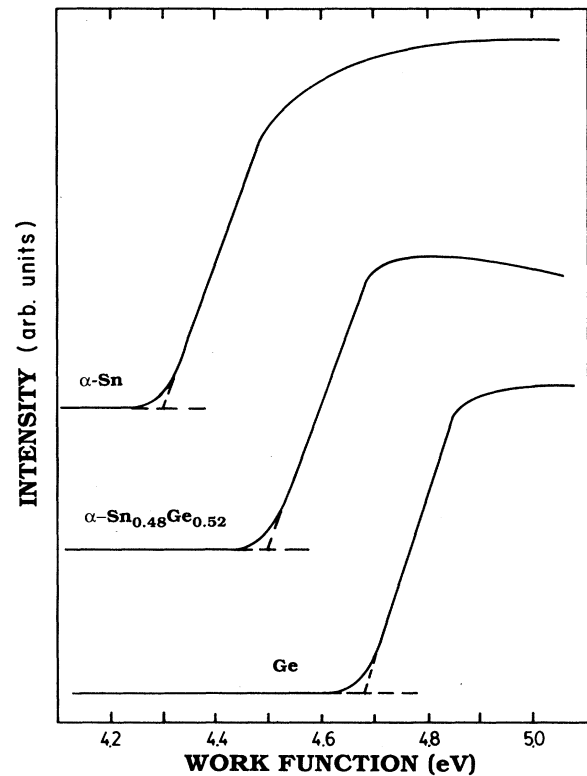
difference with thicker alloy films was an increased film roughness. These effects caused a weakening of the RHEED pattern and a reduced intensity of direct transition features in the valence-band spectra.

Another test to demonstrate the absence of larger Sn clusters in the α-Sn$_{1-x}$Ge$_x$ alloy films is given in Fig. 4, where we show the photoemission cutoff spectrum in comparison with those of α-Sn(100) and Ge(100). The position of the photoemission cutoff depends on the work function of the material, and can be easily distinguished from that of the electron analyzer by biasing the sample with a small voltage. The spectra in Fig. 4 are plotted versus the work function ϕ, which can be determined by $\phi = h\nu - E_F$. As can be seen from Fig. 4, the alloy work function agrees well with a linear model extrapolating between the work function of both alloy components. For the case of larger metallic Sn clusters on top of the Ge(100) surface, the alloy spectrum would show a stepped cutoff consisting of a superposition of the Ge and β-Sn spectra. The work function of β-Sn is ~ 0.1 eV smaller than that of the α phase[27] and should thus be easily detectable as a step in the cutoff spectrum at $\phi \sim 4.2$ eV.

Finally, we would like to discuss the issue of incorporation efficiency of the alloy components during the MBE growth. As mentioned earlier, the photoemission intensi-

ty analysis of Sn and Ge core spectra suggest that the composition of alloy films deposited at 400 °C does not linearly follow the flux composition of the molecular beam. The flux ratio of Ge/Sn has been changed by more than a factor of 10 without significant changes of the deposited alloy composition. Figure 5 shows the dependence of the alloy composition versus that of the beam. The relative concentrations were determined by normalizing the photoemission intensity of Sn $4d$ and Ge $3p$ spectra of a 200–300-Å-thick alloy film to those of bulk Sn and Ge samples. It should be noted that the core-level spectra were measured with photon energies of $h\nu \sim 35$–40 eV; they represent only the composition in the surface region (~ 15 Å), and may thus not be completely representative to the alloy composition throughout the entire film.

The question whether the additional Sn atoms which are not incorporated in the alloy lattice diffuse into the Ge substrate or reevaporate from the surface cannot be answered from our present experiments. It should be noted that DiCenzo et al.,[28] who deposited Sn on Ge(111) at room temperature, found that annealing a submonolayer to 550 °C changed the surface coverage by less then 5%. Annealing of a higher coverage, however, resulted in a stronger decrease of Sn and was attributed to reevaporation. Diffusion may also contribute to some extent to balance the missing masses but it should be kept in mind that the fairly large coefficient for substitutional diffusion of Sn into Ge ($\sim 10^{-12}$ cm^2/s at 500 °C) is most likely misleading for the present study.[29] The validity is limited since they rely on Fick's law to describe the diffusion process of impurities within the solubility limits rather than on macroscopic thick films, which, as in the present case, is not even soluble in the substrate.

The core-level analysis could rather be interpreted as a strong tendency to form a compound with a composition close to $x \sim 0.5$. The results from Shevchik and Paul,[13]
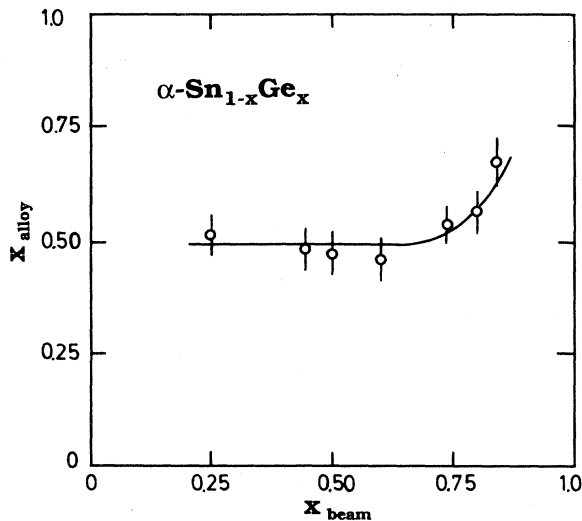

FIG. 5. Dependence of the alloy composition vs relative fluxes of the Sn and Ge molecular beams illustrating the tendency to form a SnGe compound.

who found a surprising compositional homogeneity in their sputtered SnGe compound films, already indicated the preference to form bonds with next-nearest neighbors of the opposite kind. The MBE growth of a zinc-blende-type α-SnGe compound may thus be thermodynamically more favorable than the growth of a statistically distributed substitutional diamond structured alloy.

The observed composition pinning is not unusual and has been seen previously for the coherent epitaxial growth of disordered alloys.[30−32] Various alloys of materials where the bulk constituents are immiscible have been grown as stoichiometric compounds by MBE. Recent calculations contrasting thermodynamic functions of the free energies and formation enthalpies for bulk and epitaxial growth were able to predict the observed stability of ordered epitaxial phases at growth temperatures well below the miscibility-gap temperature.[33−34]

IV. CONCLUSIONS

Alloys of α-Sn$_{1-x}$Ge$_x$ can be grown as thin films by MBE on Ge(100) substrates. ARPES and RHEED indicate good crystalline order for alloys grown at substrate temperatures $T_{\mathrm{sub}} \sim 400$ °C. However, due to a considerable lattice mismatch of $\sim 6\%$ (following Vegard's law) the alloy films show increased surface roughness which causes the transition from a typical streaked RHEED pattern to a three-dimensional bulk diffraction pattern after the deposition of the first 10–20 Å.

Compositional pinning in the epitaxial alloy was observed over a wide range of flux ratios. Core-level intensity measurements indicate a preferred growth of the alloy with $x \sim 0.5$.

Work-function measurements indicate the growth of a single-phase alloy without the precipitation of metallic tin clusters for films up to 300 Å thick.

Normal emission ARPES provides evidence of the expected band-gap closing by alloying Sn with Ge. For thin alloy films with $x \sim 0.52$ we found a shift of the valence-band maximum Γ_8 to ~ 0.16 eV below E_F. The experimental value of the Γ_8 point falls well within the expected values given by the linear band model for the alloy as well as with recent predictions based on a virtual-crystal approximation.[35] Taking into account the experimental fact that E_F does not significantly shift from its position in Ge(100), we are able to predict Γ_8 to be ~ 0.16-eV below E_F. According to the linear band model the direct gap for an alloy with $x \sim 0.52$ would be $E_g \sim 0.2$ eV, which places the bottom of the conduction band $\Gamma_7 \sim 0.04$ eV above the Fermi level.

*On leave from Dep. de Fisica, Centro de Investigacion y Estudios Avanzados del Instituto Politecnico Nacional, CINVESTAV, Mexico D.C.

[1]S. Ogus, W. Paul, T. F. Deutsch, B.-Y. Tsaur, and D. V. Murphy, Appl. Phys. Lett. **43**, 848 (1983).

[2]G. A. Busch and A. Kern, *Solid State Physics,* edited by H. Ehrenreich, F. Seitz, and D. Turnbull (Academic, New York, 1961), Vol. II, p. 1.

[3]R. F. C. Farrow, D. S. Robertson, G. M. Williams, A. G. Cullus, G. R. Jones, I. M. Young, and P. N. J. Dennis, J. Cryst. Growth **54**, 507 (1981).

[4]H. Höchst and I. Hernández-Calderón, Surf. Sci. **126**, 25 (1983).

[5]J. Menendez and H. Höchst, Thin Solid Films **111**, 375 (1984).

[6]L. Vina, H. Höchst, and M. Cardona, Phys. Rev. B **31**, 958 (1985).

[7]I. Hernández-Calderón and H. Höchst, Phys. Rev. B **25**, 4961 (1983).

[8]A. W. Ewald, J. Appl. Phys. **25**, 1436 (1954).

[9]L.-W. Tu, G. K. Wong, and J. B. Ketterson, Appl. Phys. Lett. **54**, 1010 (1989).

[10]C. A. Hoffman, J. R. Meyer, R. J. Wagner, F. J. Bartoli, M. A. Engelhardt, and H. Höchst, Phys. Rev. B (to be published).

[11]S. L. Shah, J. E. Greene, L. L. Abels, Q. Yao, and P. N. Raccah, J. Cryst. Growth **83**, 3 (1987).

[12]N. J. Shevchik and W. Paul, J. Non-Cryst. Solids **16**, 55 (1974).

[13]R. J. Temkin and W. Paul, in *Amorphous and Liquid Semiconductors,* edited by J. Stuke and W. Brenig (Taylor and Francis, London, 1974), p. 1193.

[14]I. Chambouleyron, F. C. Marques, J. P. de Souza, and I. J. R. Baumvol, J. Appl. Phys. **65**, 1591 (1989).

[15]T. C. Hsieh, T. Miller, and T.-C. Chiang, Phys. Rev. B **30**, 7005 (1984).

[16]D. H. Rich, T. Miller, and T.-C. Chiang, Phys. Rev. Lett. **60**, 357 (1988).

[17]S. D. Kevan, Phys. Rev. B **32**, 2344 (1985).

[18]J. A. Kubby, J. E. Griffith, R. S. Becker, and J. S. Vickers, Phys. Rev. B **36**, 6079 (1987).

[19]H. Höchst, D. W. Niles, and M. A. Engelhardt, SPIE Proc. **1106**, 165 (1989).

[20]I. Hernández-Calderón, D. W. Niles, and H. Höchst, J. Vac. Sci. Technol. A **6**, 1343 (1988).

[21]H. Höchst and I. Hernández-Calderón, Phys. Rev. B **40**, 8370 (1989).

[22]J. B. Bean, J. Vac. Sci. Technol. B **4**, 1427 (1986).

[23]J. R. Chelikowsky and M. L. Cohen, Phys. Rev. B **14**, 556 (1976).

[24]E. W. Plummer and W. Eberhardt, Adv. Chem. Phys. **49**, 529 (1982), and references therein.

[25]T.-C. Chiang, R. Ludeke, M. Aono, G. Landgren, F. J. Himpsel, and D. E. Eastman, Phys. Rev. B **27**, 4770 (1983).

[26]G. P. Williams, F. Cerrina, G. J. Lapeyer, J. R. Anderson, R. J. Smith, and J. Hermanson, Phys. Rev. B **34**, 5548 (1986).

[27]H. Höchst and I. Hernández-Calderón, J. Vac. Sci. Technol. A **3**, 911 (1985).

[28]S. B. DiCenzo, P. A. Bennett, D. Tribula, P. Thiry, G. K. Wertheim, and J. E. Row, Phys. Rev. B **32**, 2330 (1985).

[29]*Semiconductors, Vol. 17 of Landoldt-Börnstein,* edited by O. Madelund, M. Schulz, and H. Weiss (Springer-Verlag, Berlin, 1984), p. 118 ff.

[30]G. B. Stringfellow, J. Appl. Phys. **43**, 3455 (1972).

[31]R. F. C. Farrow, J. Vac. Sci. Technol. B **1**, 222 (1983).

[32]M. J. Jou, Y. T. Cherng, H. R. Jen, and G. B. Stringfellow, Appl. Phys. Lett. **52**, 549 (1988).

[33]D. M. Wood and A. Zunger, Phys. Rev. Lett. **61**, 1501 (1988).

[34]D. M. Wood and A. Zunger, Phys. Rev. B **38**, 12 756 (1988).

[35]D. W. Jenkins and J. D. Dow, Phys. Rev. B **36**, 7994 (1987).